

## Synthesis of Hybrid Framework Materials under “Dry” Hydrothermal Conditions: Crystal Structure and Magnetic Properties of $\text{Mn}_2(\text{H}_2\text{PO}_4)_2(\text{C}_2\text{O}_4)$

Zoe A. D. Lethbridge,<sup>†</sup> Martin J. Smith,<sup>†</sup> Satish K. Tiwary,<sup>‡</sup> Andrew Harrison,<sup>‡</sup> and Philip Lightfoot<sup>\*†</sup>

*School of Chemistry, University of St Andrews, North Haugh, St Andrews, Fife, KY16 9ST U.K.,  
Department of Chemistry, University of Edinburgh, The King's Buildings, West Mains Road,  
Edinburgh, EH9 3JJ U.K.*

Received August 15, 2003

An exploration of the manganese oxalate–phosphoric acid–water system under hydrothermal conditions, and using “reagent” quantities only of water, has led to the isolation of a new mixed anion framework material  $\text{Mn}_2(\text{H}_2\text{PO}_4)_2(\text{C}_2\text{O}_4)$ . This material features continuous chains of *cis* edge-sharing  $\text{MnO}_6$  octahedra, a motif which is unique among mixed phosphate–oxalate materials identified so far. These octahedral chains are linked into a three-dimensional framework via corner-sharing with  $\text{H}_2\text{PO}_4$  tetrahedra, with oxalate ions acting as a bis-bidentate ligand in the third direction. Magnetic susceptibility studies show that this material may be modeled as an antiferromagnetic,  $S = 5/2$  Heisenberg chain, with weaker coupling between the chains.

Hydrothermal methods provide a rich source of new materials, both in the “traditional” inorganic framework systems and, more recently, in the development of metal-organic frameworks.<sup>1</sup> These systems are synthetically complex, and although some degree of “designability” has now been introduced, particularly in metal-organic frameworks,<sup>2,3</sup> it is often not possible to predict the products of a new hydrothermal reaction with confidence. One reason for this is the wide range of synthetic variables available, including reaction time, temperature, pH, pressure, reactant source, and stoichiometry. In recent years, a new class of hybrid framework materials has been established, which consist of a combination of phosphate and oxalate ligands coordinated to metal centers. Examples now include phosphate–oxalates of both main group elements (Al, Ga, In, Sn)<sup>4</sup> and transition metals (V, Mn, Fe, Co, Mo).<sup>5</sup> Invariably, these products arise from hydrothermal reactions involving a large excess of

solvent water (typically metal/ $\text{H}_2\text{O}$  ratios less than 1:100). It has been established in zeolite chemistry that the water content itself can also be a useful synthetic variable in hydrothermal chemistry.<sup>6</sup> In the case of high-silica zeolites, a low water-content gel leads to supersaturation, and higher likelihood of producing a less thermodynamically stable (lower framework density) material due to increased “kinetic” control. In this paper, we apply similar methodology to the manganese–phosphate–oxalate system and show that new materials can also be prepared which rely on “reagent” rather than “solvent” quantities of water. Moreover, the title compound exhibits unique structural features within this family of materials, suggesting that similar methodologies may be exploited in the preparation, for example, of novel magnetic materials.

A systematic exploration of the  $\text{MnC}_2\text{O}_4 \cdot 2\text{H}_2\text{O} - \text{H}_3\text{PO}_4 - \text{H}_2\text{O}$  phase-composition diagram was carried out, comprising 12 reactions at the compositions shown in Figure 1. All reactions were carried out in 40 mL Teflon-lined stainless steel autoclaves at 160 °C for 48 h. Three different materials,  $\text{MnC}_2\text{O}_4 \cdot 2\text{H}_2\text{O}$  (JCPDS 25-544),  $\text{MnC}_2\text{O}_4 \cdot 3\text{H}_2\text{O}$  (JCPDS 32-648), and the new phase  $\text{Mn}_2(\text{H}_2\text{PO}_4)_2(\text{C}_2\text{O}_4)$  were formed, generally as mixtures, although a pure sample<sup>7</sup> of the latter was isolated from one of the reactions (i.e., reaction composition  $4\text{MnC}_2\text{O}_4 \cdot 2\text{H}_2\text{O} / 9\text{H}_3\text{PO}_4 / 7\text{H}_2\text{O}$ ).

\* To whom correspondence should be addressed. E-mail: pl@st-andrews.ac.uk.

<sup>†</sup> University of St Andrews.

<sup>‡</sup> University of Edinburgh.

(1) Cheetham, A. K.; Férey, G.; Loiseau, T. *Angew. Chem., Int. Ed.* **1999**, *38*, 3268.

(2) Férey, G. *J. Solid State Chem.* **2000**, *152*, 37.

(3) Eddaoudi, M.; Kim, J.; Rosi, N.; Vodak, D.; Wachter, J.; O’Keeffe, M.; Yaghi, O. M. *Nature* **2002**, *295*, 469.

(4) (a) Lightfoot, P.; Lethbridge, Z. A. D.; Morris, R. E.; Wragg, D. S.; Wright, P. A.; Kvik, Å.; Vaughan, G. B. M. *J. Solid State Chem.* **1999**, *143*, 74. (b) Hung, L.-C.; Kao, H.-M.; Lii, K.-H. *Chem. Mater.* **2000**, *12*, 2411. (c) Huang, J.-F.; Lii, K.-H. *J. Chem. Soc., Dalton Trans.* **1998**, *24*, 4085. (d) Natarajan, S. *J. Solid State Chem.* **1998**, *139*, 200.

(5) (a) Do, J.; Bontchev, R. P.; Jacobson, A. J. *Inorg. Chem.* **2000**, *39*, 3230. (b) Lethbridge, Z. A. D.; Tiwary, S. K.; Harrison, A.; Lightfoot, P. *J. Chem. Soc., Dalton Trans.* **2001**, 1904. (c) Choudhury, A.; Natarajan, S.; Rao, C. N. R. *Chem. Mater.* **1999**, *11*, 2316. (d) Choudhury, A.; Natarajan, S.; Rao, C. N. R. *Chem. Eur. J.* **2000**, *6*, 1168. (e) Lee, M.-Y.; Wang, S.-L. *Chem. Mater.* **1999**, *11*, 3588.

(6) Cambor, M. A.; Villaescusa, L. A.; Díaz-Cabañas, M. J. *Top. Catal.* **1999**, *9*, 59.

(7) Phase purity was established by X-ray powder diffraction on a Philips PW3710 system. Elemental analysis gave C 6.65%, H 0.93% (Calcd for  $\text{Mn}_2\text{P}_2\text{C}_2\text{H}_4\text{O}_{12}$ : C 6.13%, H 1.03%).

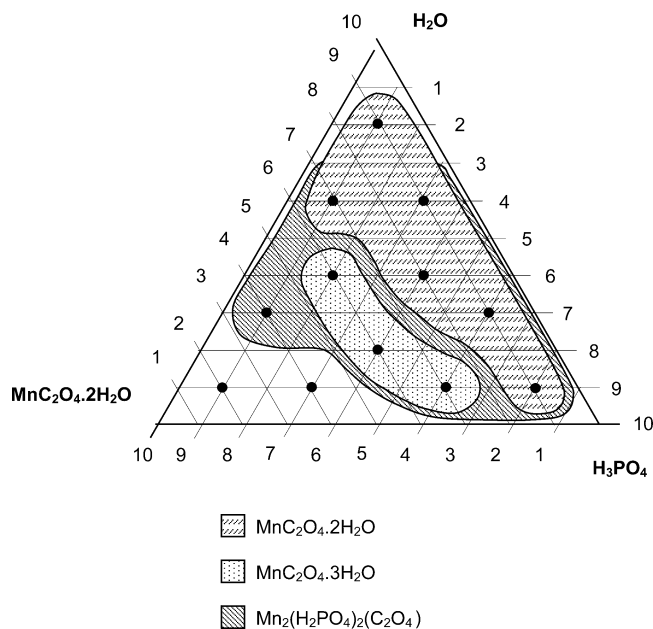


**Figure 1.** Phase-composition diagram showing the 12 reactions, and schematic product regions. Each axial “unit” corresponds to 2 mmol in the reaction mixture.

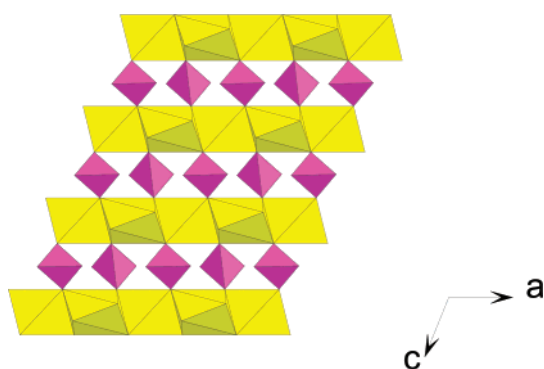


**Figure 2.** Crystal structure of  $\text{Mn}_2(\text{H}_2\text{PO}_4)_2(\text{C}_2\text{O}_4)$  showing *cis* edge-sharing chains of  $\text{MnO}_6$  octahedra linked by tetrahedral phosphate units.

Single-crystal X-ray diffraction analysis<sup>8</sup> of  $\text{Mn}_2(\text{H}_2\text{PO}_4)_2(\text{C}_2\text{O}_4)$  revealed a three-dimensional framework constructed from  $\text{MnO}_6$ ,  $\text{PO}_2(\text{OH})_2$ , and  $\text{C}_2\text{O}_4$  units. The  $\text{MnO}_6$  octahedra share *cis* edges, to form zigzag chains along the *a* axis, with a Mn–Mn distance of 3.49 Å. Neighboring chains are linked into sheets in the *ac* plane via phosphate groups (Figure 2), with these layers being linked in the *b* direction by bis-bidentate oxalate groups (Figure 3). The shortest Mn–Mn distances via these two pathways are 5.48 and 5.79 Å for phosphate and oxalate links, respectively.

Magnetic susceptibility measurements<sup>9</sup> indicate that exchange interactions are predominantly antiferromagnetic, with a cusp around 10 K (Figure 4). Octahedral  $\text{Mn}^{2+}$  should

(8) Single crystal X-ray data collection was carried out on a Bruker SMART diffractometer with a CCD detector and Mo  $K\alpha$  radiation. Structure solution and refinement were carried out using the SHELXS/SHELXL packages. All non-H atoms were refined anisotropically, with the H-atom refined isotropically. Crystal data: formula,  $\text{C}_2\text{H}_4\text{Mn}_2\text{P}_2\text{O}_{12}$ ; MW, 391.9; monoclinic, space group  $C2/m$ ;  $a = 6.045(2)$  Å,  $b = 15.064(4)$  Å,  $c = 5.511(1)$  Å,  $\beta = 112.151(4)^\circ$ ,  $V = 464.9(2)$  Å<sup>3</sup>,  $Z = 2$ ,  $T = 298$  K. Total reflections collected 1161, independent reflections 348, observed 337. Final *R* indices [ $I > 2\sigma(I)$ ]:  $R_1 = 0.023$ ,  $wR_2 = 0.061$ .

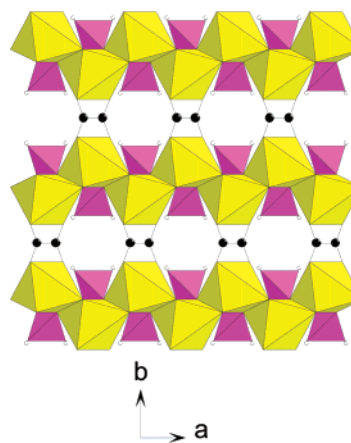


**Figure 3.** View of the  $\text{Mn}_2(\text{H}_2\text{PO}_4)_2(\text{C}_2\text{O}_4)$  structure, showing manganese phosphate layers, bridged by oxalate groups.

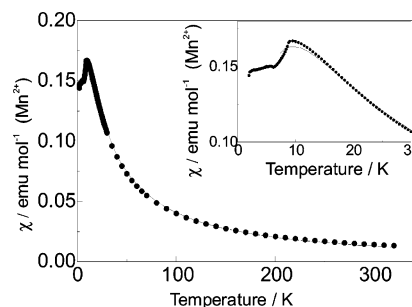


**Figure 4.** Magnetic susceptibility data for  $\text{Mn}_2(\text{H}_2\text{PO}_4)_2(\text{C}_2\text{O}_4)$  in 0.01 T field, showing the fit to the coupled-chain model (see text); the insert shows a detail of the low-temperature data.

have a  $^6A$  ground state, with  $S = 5/2$  and negligible orbital contribution to the moment, and any exchange is expected to have a Heisenberg character. Consideration of the structure in relation to likely exchange pathways suggests that the strongest interaction should be across the shared edge of the  $\text{MnO}_6$  octahedra, through two Mn–O–Mn bridges, parallel to the *a* axis; interactions mediated through oxalate anions, in a direction parallel to the *b* axis, or through phosphate anions, between the *a*–*b* planes, are likely to be weaker, but it is difficult to predict their relative strengths. Thus, to a first approximation, one might expect that the magnetic susceptibility should be described by an expression for antiferromagnetic Heisenberg chains with  $S = 5/2$ , and weaker coupling between the chains. The data were therefore fitted to the following expression:<sup>10</sup>

$$\chi = \frac{C}{T - \theta} \frac{1 - u}{1 + u} + \text{TIP}^{11}$$

A least-squares fit of this model to the data over the temperature range 7–320 K yielded optimized parameters  $g\mu_B\sqrt{S(S+1)} = 5.96(12) \mu_B$ ,  $T_0 = -13.8 (1.5) \text{ K}$  ( $J/k_B =$

(9) The magnetization was measured in applied fields of 0.01 T and 0.1 T over the temperature range 1.8–320 K, using a Quantum Design MPMS2 SQUID magnetometer, and converted to molar susceptibility. Data were corrected for the diamagnetic response of the capsule and the atoms.

(10) (a) Fisher, M. E. *Am. J. Phys.* **1964**, *32*, 343 (b) Dingle, R.; Lines, M. E.; Holt, S. L. *Phys. Rev.* **1969**, *187*, 643.

$-0.79(9)$  K),  $\theta = -2.3(1.0)$  K, and  $TIP = 0$  within experimental error (Figure 4). At temperatures below 7 K, the form of the expression deviates significantly from our measurements, which is to be expected as the temperature approaches the energy scale of interchain interactions, and the mean-field approximation breaks down. Due to the complexity of the structure, and the uncertainty in the relative strength of various possible further-neighbor interactions, it is unlikely that more meaningful interpretation of the low-temperature susceptibility can be made on the strength of these measurements.

$Mn_2(H_2PO_4)_2(C_2O_4)$  is the only phosphate–oxalate so far reported with a continuous array of edge-sharing metal–oxygen polyhedra. Edge-sharing dimers linked by corner-sharing metal polyhedra form isolated tetrameric units in  $Mn_4(PO_4)_2(C_2O_4)(H_2O)_2$ <sup>12</sup> and  $Fe_4(PO_4)_2(C_2O_4)(H_2O)_2$ .<sup>5c</sup> Edge-sharing octahedral dimers, linked through phosphate groups, occur in a related series of compounds based on  $[M_4(HPO_4)_2(C_2O_4)_3]^{2-}$  stoichiometry ( $M = Mn$ ,<sup>5b</sup>  $Fe$ ,<sup>13</sup> and  $Co$ <sup>5d</sup>). All these materials show antiferromagnetic interactions, with susceptibility maxima in the range 9–40 K. The *cis*-edge-sharing octahedral chain present in the title compound is discussed by Moore<sup>14</sup> and Hawthorne<sup>15</sup> and is present in the

mineral foggite,  $Ca[CaAl_2(OH)_4(PO_4)_2](H_2O)_2$ .<sup>16</sup> Similar chains are present in the phosphite  $Ni_{1-x}Co_x(HPO_3) \cdot H_2O$ .<sup>17</sup> In this case, the chains are further linked by corner-sharing into a continuous 2-D Ni–O network, but there are no interlayer links. The pure Ni material orders antiferromagnetically, but with evidence of ferromagnetic interactions (positive  $\theta$  value), whereas the Co containing materials are weak ferromagnets.

In conclusion, we have carried out the first systematic study of the use of variable “reagent” quantities of water in a hydrothermal “hybrid framework” system. A new manganese–phosphate–oxalate,  $Mn_2(H_2PO_4)_2(C_2O_4)$ , has been characterized. The structure exhibits, uniquely for such materials, a continuous edge-sharing octahedral metal–oxygen chain. The magnetic data suggest two distinct superexchange pathways, both intra- and interchain. Future work may exploit this methodology in different cation systems, in order to produce novel magnetic behavior.

**Acknowledgment.** We thank Dr A. M. Z. Slawin for collection of the single crystal data and the EPSRC for funding.

**Supporting Information Available:** Crystallographic data in CIF format. This material is available free of charge via the Internet at <http://pubs.acs.org>.

IC0349712

- (11) TIP is a temperature-independent contribution to the susceptibility,  $C = (N_A g^2 \mu_B^2 S(S+1)/3k_B)$ ,  $u = (T/T_0) - \coth(T_0/T)$  and  $T_0 = 2JS(S+1)/k_B$ ;  $\theta$  provides a measure of the energy scale of the mean-field coupling between the chains. Strictly speaking, the expression for the susceptibility is valid for classical (infinite) spins, but it has been shown to be a good approximation for large spins such as  $S = 5/2$  [Smith, T.; Friedberg, S. A. *Phys. Rev.* **1968**, *176*, 660].
- (12) Lethbridge, Z. A. D.; Hillier, A. D.; Cywinski, R.; Lightfoot, P. J. *Chem. Soc., Dalton Trans.* **2000**, 1595.
- (13) Choudhury, A.; Natarajan, S.; Rao, C. N. R. *J. Solid State Chem.* **1999**, *146*, 538.

- (14) Moore, P. B. *Proceedings of the 2nd International Congress on Phosphorus Compounds*; 1980, 105.
- (15) Hawthorne, F. C. *Am. Mineral.* **1985**, *70*, 455.
- (16) Moore, P. B.; Kampf, A. R.; Araki, T. *Am. Mineral.* **1975**, *60*, 965.
- (17) Marcos, M. D.; Amorós, P.; Sapiña, F.; Beltrán-Porter, A.; Martínez-Máñez, R.; Attfield, J. P. *Inorg. Chem.* **1993**, *32*, 5044.